Article

Dammarane-Type Triterpenoids from the Roots of *Rhus chinensis* and Their Preventive Effects on Zebrafish Heart Failure and Thrombosis

Miao Ye,[⊥] Wen Xu,[⊥] Da-Qing He, Xian Wu, Wen-Fang Lai, Xiao-Qin Zhang, Yu Lin, Wei Xu,* and Xu-Wen Li*

Read Online

ACCESS | Metrics & More | Article Recommendations | Supporting Information

ABSTRACT: Eight new dammarane-type triterpenoids (**1−8**), together with a related known analogue (**9**), were isolated from the roots of *Rhus chinensis*, a traditional Chinese medicine for treating coronary artery heart disease, guided by LC-MS analysis. Their structures were elucidated based on extensive spectroscopic analysis and quantum chemical calculations. Notably, compounds **1−7** and **9** possess an unusual 17α-side chain, and **1−4**, **6**, and **9** contain an uncommon 3-methyl-5,6-dihydro-2*H*-pyran-2-one moiety in the side chain. Compounds **1−5** and **9** have a 3,19-hemiketal bridge in the A ring. In an in vivo bioassay, **1**, **2**, and **4−6** exhibited significant preventive effects on zebrafish heart failure at 0.5 μg/mL, improving heart dilatation, venous congestion, cardiac output, blood flow velocity, and heart rate. Compound **5**, displaying the most promising heart failure preventive activities, showed even better effects on increasing cardiac output (72%) and blood flow velocity (83%) than six first-line heart failure therapeutic drugs. Moreover, **1**, **2**, and **6** prevented the formation of thrombosis in zebrafish at 0.5 μg/mL. The present investigation suggests that the new dammarane triterpenoids might be partially responsible for the utility of *R. chinensis* in treating coronary artery heart disease.

Rhus chinensis — Zebrafish — Preventive activity on heart failure — Anti-thrombosis activity
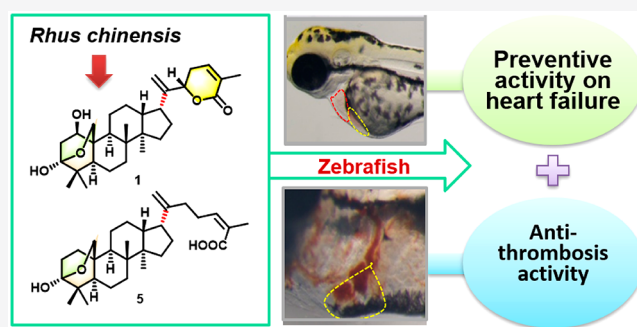
Cardiovascular disease (CVD), such as heart failure and thromboembolic conditions, remains the major reason for mortality in humans.[1] However, the limited efficacy as well as the adverse effects of current clinical drugs make the search for new cardiovascular agents urgent, with natural products being regarded as potential leads.[2] Considered as a traditional Chinese medicine (TCM) for stimulating blood circulation to dispel blood stasis,[3] the roots of *Rhus chinensis* Mill. (Anacardiaceae) are used as a raw material in the TCM preparation Shu Guan Tong Syrup [People's Republic of China, National Medical Products Administration (NMPA) approval number: GuoYaoZhunZi Z35020635], which demonstrates supporting clinical efficacy in the treatment of coronary artery heart disease (CHD).[4] However, phytochemical research on *R. chinensis* is quite limited. To date, except for several common flavonoids, phenolic acids, and some more complex phenolic substances,[3] only 12 triterpenoids[5−9] (Figure S10, Supporting Information) were previously isolated from this plant. Thus, a more-in-depth investigation of the chemical constituents in *R. chinensis* responsible for its pharmacological activity seems of significance. In this investigation, the purification of an EtOAc extract of *R. chinensis* roots resulted in the isolation of eight new dammarane triterpenoids (**1−8**) and one known biogenetically

related compound (**9**) (Figure 1). It is worth noting that **1−7** and **9** possess a rare 17α-side chain, which has only been found in five previously reported dammarane triterpenoids in Nature.[6,10−12]

In the present study, the preventive effects of compounds on heart failure and thrombosis were assessed in zebrafish (*Danio rerio*) models. Zebrafish's close physiological similarities with humans, high fertility rate, rapid development, and transparent embryos make it a favorable model organism for utilization in the laboratory screening of new cardiovascular drugs.[13] After being treated with 200 μM verapamil (a heart failure-inducing drug) for 0.5 h, zebrafish develop symptoms such as pericardial edema, venous blood congestion, circulation defects, and bradycardia.[14] In turn, exposure to 4 μg/mL ponatinib for 18 h led to vascular occlusion in zebrafish.[15,16] These symptoms closely resemble those observed in human CVD patients. Furthermore, zebrafish heart failure and thrombosis models have been validated with several FDA or NMPA-approved
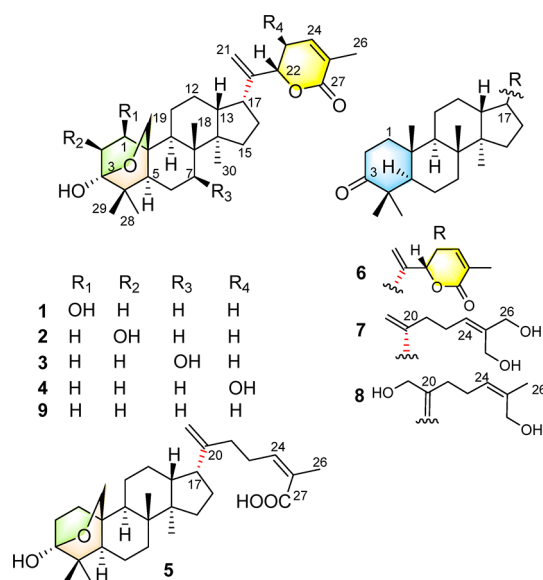
Figure 1. Structures of compounds **1−9**.

cardiovascular drugs.[14,15] Accordingly, these two models seem useful and reliable for the in vivo evaluation of the preventive and therapeutic effects of compounds on heart failure and thrombosis.

Except for a variety of fatty acids, the total ion chromatogram (TIC) of the EtOAc portion of *R. chinensis* roots revealed a number of peaks displaying similar molecular weights (e.g., *m/z* 456, 458, 468, 470, 474, 484, 486; Figure S12 and Table S1, Supporting Information) as the reported triterpenoids from *R. chinensis*[5−9] and those with a 3,19-hemiketal moiety in the A ring from the family Anacardiaceae[5−7,17−20] (Figures S10 and S11, Supporting Information). Therefore, LC-MS guided isolation targeting triterpenoids enabled the rapid purification of nine triterpenoids (**1−9**) (Figure 1). Herein, the LC-MS-guided isolation, structural elucidation, and plausible biosynthetic pathways as well as the assessment of preventive effects on zebrafish heart failure and thrombosis of the compounds are reported.

RESULTS AND DISCUSSION

Structure Elucidation of Compounds 1−9. The formula of the known compound **9** was deduced as $C_{30}H_{44}O_4$ by HRESIMS data at *m/z* 491.3169 [M + Na]$^+$ (calcd for $C_{30}H_{44}O_4Na$, 491.3137). The NMR data of **9** (Tables 1 and 2) were almost identical with two previously reported dammarane triterpenoids, semialactone[5] and rhuslactone,[6] which possess the same planar structure but opposite configurations at C-17. The relative configuration of C-17 in compound **9** was elucidated by calculation of the distance of H-21b and Me-30 assisted by NOESY experiment. First, a clear NOE cross-peak of H-21b/Me-30 in **9** was observed, which can be used as a key clue for further calculations.[21] The Boltzmann-averaged distances between H-21b and Me-30 of a pair of C-17 epimers of **9** (**9a**, **9c**; Figure 2) were calculated, with that of (3S,5S,8R,9S,10R,13R,14R,17R,22S)-**9a** with a 17α-side chain calculated to be 2.05 Å, while that of (3S,5S,8R,9S,10R,13R,14R,17S,22S)-**9c** with a 17β-side chain gave 5.06 Å. The calculations were based on the optimized geometry of conformers at the B3LYP/6-31G* level of theory (Table S2, Supporting Information). The experimental distance of H-

21b/Me-30 ($r_{H-21b/Me-30}$) in **9** was calculated as 2.21 Å, referenced to the NOE cross-peak volume (a_{ref}) and atomic distance (r_{ref} 2.53 Å) of H-1β/H-19b (Figures 3 and S9N, Supporting Information) by the formula $r_{H-21b/Me-30} = r_{ref}(a_{ref}/a_{H-21/Me-30})^{1/6}$.[21] The experimental value of $r_{H-21b/Me-30}$ was in good accordance with the theoretical value of **9a** rather than that of **9c**. Therefore, the side chain connected to C-17 was assigned as being α-oriented in **9**.

In order to determine the absolute configuration of C-17 in **9**, calculations of the ^{13}C NMR data of the four C-17 and C-22 diastereomers of **9** (**9a−9d**, Figure 2) were performed at ωB97x-D/6-31G*//B3LPY/6-31G* using the procedure and scaled parameters reported in the literature.[22] The scaled DP4+ (sDP4+) probabilities[23] of the four C-17 and C-22 diastereomers (**9a−9d**) were calculated (Table 3), which showed that the probability of a 17R-substituent was much greater than that of a 17S-substituent. Accordingly, the configuration of C-17 in **9** was determined as R. However, the differences of the sDP4+ probabilities between **9a** and **9b** were not sufficient to distinguish them. Thus, in order to assign the absolute configuration of C-22, electronic circular dichroism (ECD) calculations of **9a** and **9b** were performed. As presented in Figure 4A, the calculated ECD curve of (3S,5S,8R,9S,10R,13R,14R,17R,22S)-**9a** matched closely to the experimental data, supporting a 22S configuration. Accordingly, **9** was established as rhuslactone, for which the configuration was confirmed by single-crystal X-ray crystallographic analysis.[6] The ^1H and ^{13}C NMR data of rhuslactone (**9**) were assigned completely for the first time according to the comprehensive analysis of its $^1H−^1H$ COSY, HSQC, HMBC, and NOESY data (Tables 1 and 2).

The molecular formula of **1**, $C_{30}H_{44}O_5$, with nine degrees of unsaturation, was deduced from the positive HRESIMS (*m/z* 507.3076, calcd 507.3086). The ^1H NMR spectrum indicated the presence of four singlet methyl groups at δ 0.86, 0.89, 1.00, and 1.06 (each 3H, s, H$_3$-18, 30, 28, 29), a vinyl methyl group at δ 1.92 (3H, m, H$_3$-26), a hydroxymethylene group [δ 4.23 (dd, J = 9.1, 2.8 Hz), δ 3.69 (dd, J = 9.0, 2.0 Hz), H$_2$-19], two oxymethine groups [δ 3.99 (dd, J = 9.8, 4.1 Hz, H-1); δ 4.74 (dd, J = 12.4, 3.6 Hz, H-22)], an exomethylene group [δ 5.26 and 5.22 (each 1H, br s, H$_2$-21)], and an olefinic proton at δ 6.60 (dq, J = 6.1, 2.0 Hz, H-1) (Table 1). The ^{13}C NMR and DEPT-135 spectra revealed a total of 30 carbon signals, comprising five sp^3 methyls, nine sp^3 and one sp^2 methylene, six sp^3 and one sp^2 methine, and eight quaternary carbons (including an ester carbonyl group at δ 166.1 and a hemiketal carbon at δ 98.0; Table 2). The NMR data of **1** were almost identical to those of rhuslactone (**9**). The only difference between them was the presence of an additional hydroxy group in **1**, which was in agreement with the 16 mass units greater molecular weight than **9**. Further $^1H−^1H$ COSY and HMBC correlations shown in Figure 5 were used to confirm the planar structure of **1**. In particular, the location of the hydroxy group was shown to be at the C-1 position by the HMBC correlations from H-2β to C-1/C-5/C-10 and from H-2α to C-3/C-10, as well as the $^1H−^1H$ COSY correlations of H-1/H$_2$-2 in **1**. Further, the diagnostic $^1H−^1H$ COSY correlations of H-22/H$_2$-23/H-24 along with the key HMBC correlations from H-23a to C-22/C-24/C-25, from H-24 to C-22/C-23/C-25/C-26/C-27, and from H$_3$-26 to C-24/C-25/C-27 were consistent with the presence of an unusual 3-methyl-5,6-dihydro-2H-pyran-2-one moiety. The occurrence of a characteristic hemiketal moiety (δ 98.0, C-3; δ 67.8, CH$_2$-19) in the

Table 1. ^{1}H NMR Data of Compounds 1−9 (500 MHz, CDCl$_3$)

no.	1	2	3	4	5	6	7	8	9
1α	3.99, dd (9.8, 4.1)	1.21, dd, oᵃ	1.09, m	1.12, m	1.13, m	1.41, m	1.41, m	1.48, m	1.12, m
1β		2.41, br d, 14.5	2.21, m	2.19, m	2.21, m	1.91, m	1.91, m	1.93, m	2.18, m
2α	1.76, dd, oᵃ	3.37, br s	2.17, m	2.15, m	2.16, m	2.44, m	2.45, m	2.48, m	2.15, m
2β	1.91, dd, oᵃ		1.68, m	1.66, m	1.64, m	2.44, m	2.45, m	2.48, m	1.70, m
5α	1.15, m	1.23, m	1.36, m	1.21, m	1.21, m	1.40, m	1.36, m	1.41, m	1.21, m
6α	1.47, m	1.53, m	2.01, m	1.47, m	1.71, m	1.47, m	1.46, m	1.51, m	1.45, m
6β	1.65, m	1.53, m	2.01, m	1.64, m	1.42, m	1.54, m	1.46, m	1.51, m	1.63, m
7α	1.47, m	1.54, m	3.74, dd (11.9, 4.1)	1.48, m	1.46, m	1.57, m	1.54, m	1.55, m	1.47, m
7β	1.29, m	1.32, m		1.29, m	1.27, m	1.29, m	1.27, m	1.38, m	1.28, m
9α	1.42, dd, oᵃ	1.75, dd, oᵃ	1.37, dd, oᵃ	1.44, dd, oᵃ	1.45, dd, oᵃ	1.44, dd, oᵃ	1.39, dd, oᵃ	1.47, dd, oᵃ	1.44, dd, oᵃ
11α	1.07, m	1.19, m	1.27, m	1.05, m	1.02, m	1.27, m	1.24, m	1.32, m	1.05, m
11β	1.61, m	1.77, m	1.68, m	1.66, m	1.65, m	1.54, m	1.53, m	1.58, m	1.63, m
12α	1.22, m	1.26, m	1.22, m	1.21, m	1.21, m	1.24, m	1.24, m	1.46, m	1.21, m
12β	1.64, m	1.66, m	1.62, m	1.69, m	1.70, m	1.64, m	1.69, m	2.26, m	1.62, m
13β	2.11, ddd (13.7, 11.1, 3.3)	2.14, ddd (15.9, 11.8, 4.1)	2.07, ddd (12.0, 9.7, 3.2)	2.14, ddd, oᵃ	2.02, ddd, oᵃ	2.14, ddd (12.0, 10.1, 3.0)	2.03, ddd, oᵃ	2.41, m, oᵃ	2.11, ddd, oᵃ
15α	1.29, m	1.32, m	1.71, m	1.29, m	1.27, m	1.29, m	1.24, m	1.59, m	1.28, m
15β	1.47, m	1.51, m	1.54, m	1.48, m	1.49, m	1.57, m	1.54, m	1.59, m	1.47, m
16α	1.72, m	1.74, m	1.72, m	1.67, m	1.80, m	1.74, m	1.79, m	1.21, m	1.71, m
16β	1.96, m	1.95, m	1.95, m	1.97, m	2.63, m	1.94, m	1.79, m	1.21, m	1.95, m
17α									
17β	2.96, br dd (10.6, 8.5)	2.98, br dd (11.3, 10.7)	2.90, br dd (10.0, 8.0)	2.94, br dd (11.1, 8.7)	2.64, m	2.98, br dd (9.2, 7.8)	2.61, m		2.95, br dd (12.7, 11.5)
18	0.86, s	0.76, s	0.88, s	0.88, s	0.85, s	0.99, s	0.97, s	1.02, s	0.87, s
19a	4.23, dd (9.1, 2.8)	3.83, dd (10.4, 1.7)	4.18, dd (8.9, 2.9)	4.22, dd (8.9, 2.9)	4.24, dd (11.0, 3.6)	0.94, 3H, s	0.93, 3H, s	0.95, 3H, s	4.23, dd (11.0, 3.5)
19b	3.69, dd (9.0, 2.0)	3.79, br d (10.5)	3.72, dd (9.2, 2.8)	3.72, dd (8.9, 2.0)	3.73, dd (11.1, 2.4)				3.72, dd (11.0, 2.5)
21a	5.26, br s	5.28, d, 1.1	5.26, br s	5.34, br s	4.92, br s	5.26, br s	4.95, br s	4.07, 2H, br s	5.25, br s
21b	5.22, br s	5.24, d, 1.5	5.21, br s	5.28, br s	4.88, br s	5.23, br s	4.87, br s		5.22, br s
22a	4.74, dd (12.4, 3.6)ᶜ	4.76, dd (15.5, 4.5)ᶜ	4.75, dd (12.5, 3.6)ᶜ	4.54, d (9.4)ᶜ	2.16, m	4.76, dd (10.5, 3.0)ᶜ	2.13, m	2.33, m	4.74, dd (15.5, 4.5)ᶜ
22b					2.04, m		2.00, m	2.33, m	
23a	2.53, m	2.54, m	2.52, m	4.45, dt (9.4, 2.2)ᵇ	2.68, m	2.54, m	2.21, m	2.17, m	2.52, m
23b	2.34, m	2.36, m	2.32, m		2.58, m	2.34, m	2.21, m	2.17, m	2.33, m
24	6.60, dq (6.1, 2.0)	6.61, dq (6.9, 2.0)	6.60, dq (5.7, 1.8)	6.56, br q (2.0)	6.06, tq (9.3, 2.1)	6.60, dq (5.6, 1.5)	5.54, t (8.7)	5.33, br d (7.5)	6.59, dq (7.1, 2.2)
26	1.92, 3H, m	1.92, 3H, m	1.92, 3H, m	1.93, 3H, t (1.8)	1.90, 3H, m	1.90, 3H, m	4.20, 2H, s	1.80, 3H, br s	1.92, 3H, m
27							4.29, 2H, s	4.09, 2H, br s	
28	1.00, s	1.10, s	1.04, s	1.02, s	1.02, s	1.08, s	1.07, s	1.08, s	1.02, s
29	1.06, s	0.98, s	1.00, s	0.97, s	0.98, s	1.04, s	1.03, s	1.04, s	0.98, s
30	0.89, s	0.90, s	0.99, s	0.93, s	0.85, s	0.92, s	0.88, s	0.82, s	0.89, s

ᵃ"o" is used to indicate overlapping signal, for which the coupling constants could not be read. ᵇProton α-oriented. ᶜProton β-oriented.

A ring was confirmed by the HMBC correlations from H-19b to C-3/C-5/C-10 and from H-2/H$_3$-28/H$_3$-29 to C-3 (Figure 5).

The relative configuration of the A, B, C, and D rings of **1** was deduced to be the same as those of **9** based on biogenetic considerations and was confirmed by a NOESY experiment (Figure 5). The α-orientations of H-5, H-9, H$_3$-28, and H$_3$-30 in **1** were ascertained by the NOESY correlations of H$_3$-28α/ H-5, H-5/H-9, and H-9/H$_3$-30. In turn, the β-orientations of H-13, H$_3$-18, H$_2$-19, and H$_3$-29 were substantiated by the NOE cross-peaks of H$_3$-29β/H$_2$-19, H$_2$-19/H$_3$-18, and H$_3$-18/ H-13. Due to the rigid nature of the hemiketal bridge between C-3 and C-19, OH-3 was assigned with an α-orientation. The β-orientation of OH-1 was determined by the large value of $J_{H-1,2}$ (9.8 Hz) along with the clear NOESY correlation of H-1/ H$_3$-28α (Figure 5).

Similar to **9**, on the basis of the aforementioned equation $[r_{H-21b/Me-30} = r_{ref}(a_{ref}/a_{H-21/Me-30})^{1/6}]$,[21] the experimental dynamic distance of H-21b/Me-30 in **1** was calculated to be 2.51 Å, according to its NOE strength relative to the protons on a rigid structure (H-1α/H-2α) (Figure S1N, Supporting Information). Furthermore, except for C-1 and C-2, the ^{13}C NMR data of **1** were almost the same as those of **9**. Thus, based on the calculated atom distance of H-21b/Me-30 and the ^{13}C NMR data, a 17R configuration in **1** was established. In an ECD experiment of **1**, negative π−π* Cotton effects at 199

Table 2. ^{13}C NMR and DEPT-135 Data for Compounds 1−9 (125 MHz, CDCl$_3$)

no.	1	2	3	4	5	6	7	8	9
1	68.2, CH	45.8, CH$_2$	35.4, CH$_2$	35.7, CH$_2$	35.7, CH$_2$	40.1, CH$_2$	40.0, CH$_2$	40.1, CH$_2$	35.7, CH$_2$
2	47.5, CH$_2$	82.0, CH	29.6, CH$_2$	29.7, CH$_2$	29.7, CH$_2$	34.6, CH$_2$	34.2, CH$_2$	34.2, CH$_2$	29.7, CH$_2$
3	98.0, C	102.5, C	98.5, C	98.3, C	98.9,^{a} C	218.2, C	218.4, C	218.2, C	98.4,^{a} C
4	39.1, C	48.2, C	40.4, C	40.6, C	40.6, C	47.6, C	47.6, C	47.5, C	40.7, C
5	49.7, CH	54.8, CH	48.4, CH	50.2, CH	50.0, CH	55.6, CH	55.4, CH	55.4, CH	50.2, CH
6	19.8, CH$_2$	20.6, CH$_2$	31.2, CH$_2$	20.1, CH$_2$	20.0, CH$_2$	19.9, CH$_2$	19.8, CH$_2$	19.8, CH$_2$	20.0, CH$_2$
7	33.2, CH$_2$	34.3, CH$_2$	73.6, CH	33.5, CH$_2$	33.2, CH$_2$	34.3, CH$_2$	34.4, CH$_2$	34.9, CH$_2$	33.3, CH$_2$
8	39.8, C	40.1, C	45.4, C	40.0, C	39.7, C	40.9, C	40.8, C	39.9, C	39.9, C
9	45.4, CH	43.5, CH	45.6, CH	45.6, CH	45.5, CH	50.4, CH	50.3, CH	50.1, CH	45.6, CH
10	36.1, C	39.9, C	35.5, C	35.6, C	35.6, C	37.0, C	37.0, C	36.9, C	35.7, C
11	23.3, CH$_2$	22.9, CH$_2$	23.2, CH$_2$	23.3, CH$_2$	23.3, CH$_2$	22.6, CH$_2$	22.6, CH$_2$	22.3, CH$_2$	23.3, CH$_2$
12	25.4, CH$_2$	25.1, CH$_2$	25.3, CH$_2$	25.3, CH$_2$	25.5, CH$_2$	25.2, CH$_2$	25.2, CH$_2$	26.9, CH$_2$	25.5, CH$_2$
13	45.1, CH	45.2, CH	46.1, CH	45.3, CH	45.2, CH	45.0, CH	45.0, CH	47.6, CH	45.2, CH
14	49.5, C	49.1, C	48.6, C	49.4, C	49.6, C	49.9, C	50.0, C	49.6, C	49.5, C
15	33.1, CH$_2$	33.4, CH$_2$	36.8, CH$_2$	33.4, CH$_2$	33.1, CH$_2$	33.3, CH$_2$	33.2, CH$_2$	30.2, CH$_2$	33.3, CH$_2$
16	30.3, CH$_2$	30.0, CH$_2$	29.8, CH$_2$	31.6, CH$_2$	28.8, CH$_2$	30.4, CH$_2$	28.3, CH$_2$	29.8, CH$_2$	30.3, CH$_2$
17	40.1, CH	40.2, CH	38.9, CH	39.5, CH	43.8, CH	40.2, CH	44.1, CH	142.7, C	40.2, CH
18	15.6, CH$_3$	15.2, CH$_3$	9.9, CH$_3$	15.6, CH$_3$	15.6, CH$_3$	15.7, CH$_3$	15.6, CH$_3$	15.5, CH$_3$	15.6, CH$_3$
19	67.8, CH$_2$	67.9, CH$_2$	67.8, CH$_2$	68.2, CH$_2$	68.3, CH$_2$	16.2, CH$_3$	16.2, CH$_3$	16.4, CH$_3$	68.1, CH$_2$
20	149.4, C	149.3, C	149.4, C	147.1, C	151.5, C	149.3, C	151.6, C	130.5, C	149.4, C
21	113.6, CH$_2$	113.6, CH$_2$	113.9, CH$_2$	116.5, CH$_2$	109.8, CH$_2$	113.7, CH$_2$	109.7, CH$_2$	65.0, CH$_2$	113.6, CH$_2$
22	81.0, CH	80.8, CH	81.2, CH	86.4, CH	38.0, CH$_2$	81.1, CH	38.3, CH$_2$	28.5, CH$_2$	81.0, CH
23	29.2, CH$_2$	29.1, CH$_2$	29.4, CH$_2$	64.9, CH	28.2, CH$_2$	29.1, CH$_2$	26.7, CH$_2$	28.4, CH$_2$	29.2, CH$_2$
24	139.3, CH	139.3, CH	139.2, CH	142.5, CH	146.0, CH	139.3, CH	130.8, CH	128.5, CH	139.3, CH
25	128.6, C	128.6, C	128.6, C	128.1, C	126.4, C	128.6, C	137.4, C	134.9, C	128.6, C
26	17.2, CH$_3$	17.2, CH$_3$	17.2, CH$_3$	16.9, CH$_3$	20.7, CH$_3$	17.2, CH$_3$	60.2, CH$_2$	21.7, CH$_3$	17.2, CH$_3$
27	166.1, C	166.2, C	166.1, C	164.6, C	172.4, C	166.2, C	67.7, CH$_2$	61.7, CH$_2$	166.1, C
28	26.6, CH$_3$	31.3, CH$_3$	26.9, CH$_3$	27.0, CH$_3$	26.9, CH$_3$	26.8, CH$_3$	26.9, CH$_3$	26.9, CH$_3$	27.0, CH$_3$
29	18.9, CH$_3$	15.7, CH$_3$	18.7, CH$_3$	18.6, CH$_3$	18.6, CH$_3$	21.2, CH$_3$	21.1, CH$_3$	21.1, CH$_3$	18.6, CH$_3$
30	16.7, CH$_3$	16.8, CH$_3$	16.4, CH$_3$	17.0, CH$_3$	16.5, CH$_3$	17.1, CH$_3$	16.9, CH$_3$	16.7, CH$_3$	16.7, CH$_3$

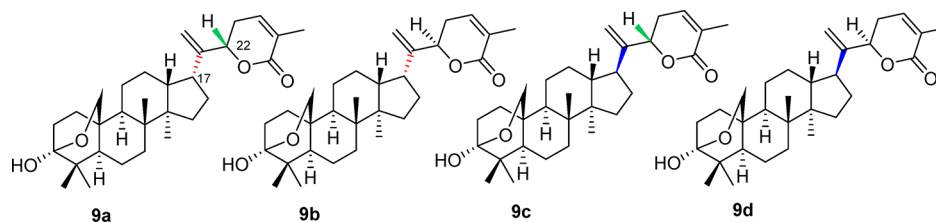^{a}Signals were determined using HMBC correlations.

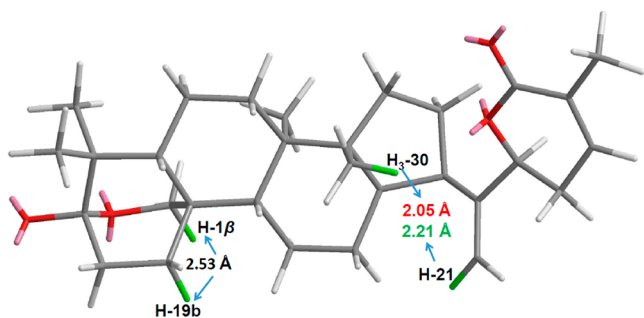**Figure 2.** Structures of four C-17 and C-22 diastereomers of compound **9**.

Figure 3. Theoretical (calculated by DFT, red) and experimental (calculated by NOE intensity, green) dynamic distances of H-21b/Me-30 of compound **9**.

and 255 nm were apparent, and the band shape was nearly the same as that of **9** (Figure 4B). Hence, a 22S configuration was

assigned, and compound **1** was defined as 1β-hydroxyrhus-lactone.

Compound **2** was assigned with the same molecular formula of $C_{30}H_{44}O_5$ as **1** on the basis of the HRESIMS ion peak at m/z 507.3076 [M + Na]$^+$ (calcd for $C_{30}H_{44}O_5Na$, 507.3086). The ^{13}C NMR data (Table 2) of rings C and D and the lactone of **2** were nearly the same as those of **1**, suggesting the only difference between them was the location of a hydroxy group in the A ring. The hydroxy group in **2** was located at C-2 (δ 82.0) by the HMBC correlations between H-2 (δ 3.37) and C-1/C-3/C-28/C-29. The broad single peak of the H-2 resonance in the ^{1}H NMR spectrum as well as the NOESY correlations of H-19b (δ 3.79)/H$_3$-29β (δ 0.98) and H$_3$-28α (δ 1.10)/H-2 supported an α-equatorial orientation of H-2. The value of $r_{H-21/Me-30}$ (2.11 Å) was calculated in the same way as that for **1** (Figure S2M, Supporting Information), which was closely comparable to that of **1**. As a result, a 17R configuration in **2** was determined. The 22S configuration was deduced

Table 3. Experimental ^{13}C NMR Data (CDCl$_3$) of 9 and Calculated ^{13}C NMR Data of Four Diastereomers of 9 (9a−9d)

no.	exptl.	9a	deviation	9b	deviation	9c	deviation	9d	deviation
1	35.7	36.6	−0.9	36.7	−1.0	36.8	−1.1	36.7	−1.0
2	29.7	28.8	0.9	28.7	1.0	28.8	0.9	28.8	0.9
3	98.4	99.2	−0.8	99.1	−0.7	99.1	−0.7	99.2	−0.8
4	40.7	42.8	−2.1	43.0	−2.3	43.1	−2.4	43.1	−2.4
5	50.2	50.2	0.0	50.0	0.2	50.1	0.1	50.3	−0.1
6	20.0	21.9	−1.9	21.8	−1.8	21.8	−1.8	21.9	−1.9
7	33.3	34.4	−1.1	34.9	−1.6	35.3	−2.0	35.3	−2.0
8	39.9	42.4	−2.5	42.3	−2.4	42.1	−2.2	42.1	−2.2
9	45.6	46.4	−0.8	46.3	−0.7	46.3	−0.7	46.4	−0.8
10	35.7	36.6	−0.9	36.7	−1.0	36.6	−0.9	36.7	−1.0
11	23.3	24.8	−1.5	25.0	−1.7	24.2	−0.9	24.3	−1.0
12	25.5	24.9	0.6	25.7	−0.2	25.7	−0.2	25.9	−0.4
13	45.2	48.1	−2.9	47.6	−2.4	45.7	−0.5	53.0	−7.8
14	49.5	51.3	−1.8	51.3	−1.8	51.1	−1.6	51.4	−1.9
15	33.3	35.0	−1.7	34.7	−1.4	32.4	0.9	33.4	−0.1
16	30.3	33.3	−3.0	32.4	−2.1	32.3	−2.0	34.0	−3.7
17	40.2	39.7	0.5	41.6	−1.4	43.1	−2.9	42.6	−2.4
18	68.1	68.1	0.0	68.2	−0.1	68.2	−0.1	68.2	−0.1
19	15.6	16.4	−0.8	17.3	−1.7	17.3	−1.7	17.2	−1.6
20	149.4	152.8	−3.4	152.3	−2.9	152.7	−3.3	155.3	−5.9
21	113.6	115.2	−1.6	115.4	−1.8	112.1	1.5	115.5	−1.9
22	81.0	82.4	−1.4	81.8	−0.8	78.2	2.8	81.4	−0.4
23	29.2	31.1	−1.9	31.2	−2.0	26.7	2.5	30.3	−1.1
24	139.3	138.7	0.6	138.3	1.0	137.2	2.1	138.6	0.7
25	128.6	131.8	−3.2	132.3	−3.7	132.4	−3.8	132.1	−3.5
26	17.2	19.0	−1.8	19.1	−1.9	19.3	−2.1	19.0	−1.8
27	166.1	162.3	3.8	162.9	3.2	161.6	4.5	162.5	3.6
28	27.0	27.2	−0.2	27.1	−0.1	27.1	−0.1	27.1	−0.1
29	18.6	19.5	−0.9	19.5	−0.9	19.6	−1.0	19.7	−1.1
30	16.7	18.2	−1.5	17.7	−1.0	16.2	0.5	16.4	0.3
		MAE	1.50	MAE	1.49	MAE	1.59	MAE	1.75
		RMS	1.80	RMS	1.74	RMS	1.94	RMS	2.45
		sDP4+	44.3%	sDP4+	51.4%	sDP4+	4.01%	sDP4+	0.24%
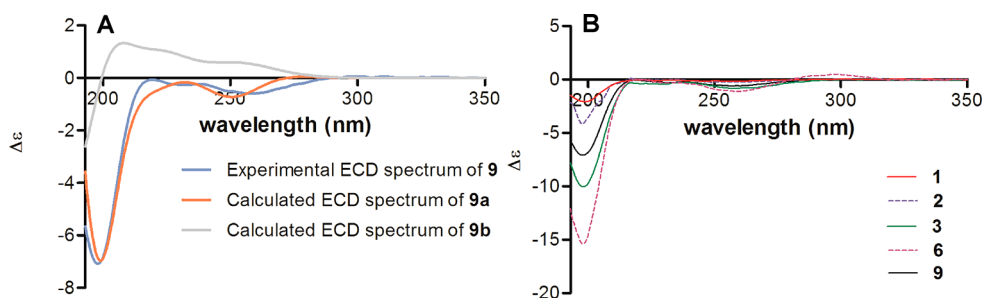
Figure 4. (A) Experimental ECD spectrum of **9** (blue) and the calculated ECD spectra of (3*S*,5*S*,8*R*,9*S*,10*R*,13*R*,14*R*,17*R*,22*S*)-**9a** (red) and (3*S*,5*S*,8*R*,9*S*,10*R*,13*R*,14*R*,17*R*,22*R*)-**9b** (gray). (B) Experimental ECD spectra of **1** (red, continuous line), **2** (blue, dashed line), **3** (green, continuous line), **6** (purple, dashed line), and **9** (black, continuous line).

based on the similar ECD curve of **2** to that of **1** (Figure 4B). Accordingly, **2** was elucidated as 2*β*-hydroxyrhuslactone.

The ^{13}C NMR spectrum of compound **3** revealed that it coexisted with an uncharacterized impurity, which did not influence the elucidation of its structure. Compound **3** was deduced as an isomer of **1** and **2** from the HRESIMS data (*m/z* 507.3076 [M + Na]$^+$, calcd 507.3086). Further 1D and 2D NMR spectra comparison indicated that the only difference between them was the location of the hydroxy group (Tables 1 and 2). The HMBC correlations of H-5, H$_2$-6, H-9, H$_3$-18/C-7 and H-7/C-18 proved that C-7 (*δ* 73.6) was hydroxylated. The *α*-axial orientation of H-7 was interpreted by a large value of

$J_{H-6,7}$ (11.9 Hz) as well as the NOE cross-peak of H-7/H$_3$-30*α*. Close similarities in the experimental distance of H-21b/Me-30 (2.11 Å, Figure S3Q, Supporting Information) and the ECD data with compounds **1**, **2**, and **9** (Figure 4B) permitted the assignment of the absolute configurations of C-17 and C-22 as *R* and *S*, respectively. As a result, **3** was determined as 7*β*-hydroxyrhuslactone.

The molecular formula of compound **4** was identical to those of **1**−**3**, as supported by the HRESEMS and NMR data. The A to D rings exhibited nearly identical NMR data (Tables 1 and 2) to those of **9**, indicating that the hydroxy group might be located on the lactone ring. The HMBC correlations
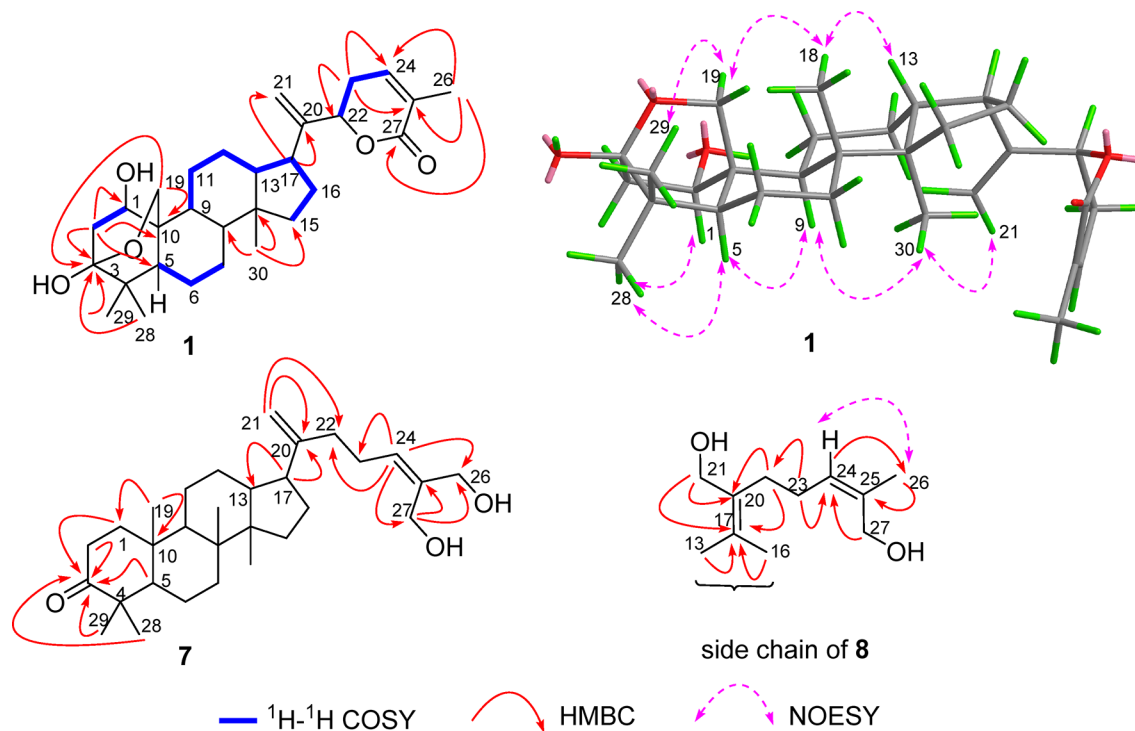
Figure 5. Key 2D NMR correlations of **1**, **7**, and **8**.

between H-23 and C-20/C-21/C-22/C-24 and H-21b/H-22/H$_3$-26 and C-23, as well as the ^{1}H−^{1}H COSY correlations of H-23/H-24/H$_3$-26, were used to place the hydroxy group at C-23. By comparing the ^{13}C NMR data of the A to D ring moieties as well as the experimental distance between H-21b and Me-30 (2.13 Å, Figure S4M, Supporting Information) with those of **9**, a 17*R* configuration for **4** was established. The large coupling constant ($J_{H-22,23}$ = 9.4 Hz) between H-22 and H-23 indicated that they were both in the axial positions. Thus, H-22 and H-23 were on the opposite sides of the lactone. In order to define the absolute configurations of C-22 and C-23, the calculated ECD spectra of (3*S*,5*S*,8*R*,9*S*,10*R*,13*R*,-14*R*,17*R*,22*S*,23*R*)-**4** and (3*S*,5*S*,8*R*,9*S*,10*R*,13*R*,-14*R*,17*R*,22*R*,23*S*)-**4** were obtained. The experimental ECD spectrum of **4** was in good accordance with the calculated spectrum for (3*S*,5*S*,8*R*,9*S*,10*R*,13*R*,14*R*,17*R*,22*S*,23*R*)-**4**, showing two large negative π−π* Cotton effects at 198 and 263 nm and a positive one at 226 nm. In turn, the ECD spectrum of (3*S*,5*S*,8*R*,9*S*,10*R*,13*R*,14*R*,17*R*,22*R*,23*S*)-**4** demonstrated large negative π−π* Cotton effects at 201 and 240 nm and positive ones at 214 and 263 nm, quite different from the experimental ECD data of **4** (Figure 6). Therefore, the absolute configurations 17*R*, 22*S*, 23*R* could be proposed, and **4** was established as (23*R*)-23-hydroxyrhuslactone.

The elemental formula of compound **5** was deduced as C$_{30}$H$_{46}$O$_4$ from the positive-ion peak at *m/z* 471.3499 [M + H]$^+$ (calcd 471.3474), exhibiting eight degrees of unsaturation, one less than that of **9**. The A to D rings of **5** displayed very similar NMR data (Tables 1 and 2) to those of **9**. Therefore, these compounds were considered to contain different side chains. The ^{13}C and DEPT-135 NMR spectra of **5** revealed that its side chain contains an ester carboxyl group at δ 172.4 and two double bonds (δ 109.8 and 151.5; δ 146.0 and 126.4). Accordingly, the lactone ring was found to be opened in **5**. The HMBC correlations of H-17/C-13, C-20, and C-21 and H$_2$-
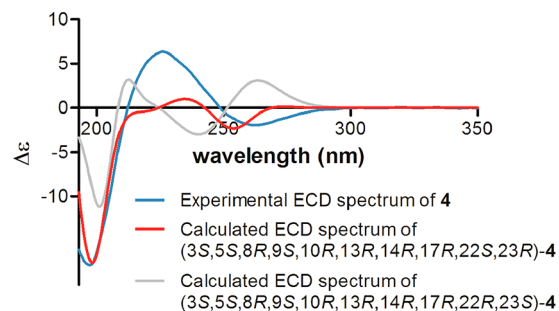

Figure 6. Experimental ECD spectrum of (23*R*)-23-hydrxoylrhus-lactone (**4**) (blue) and the calculated ECD spectra of (3*S*,5*S*,8*R*,9*S*,10*R*,13*R*,14*R*,17*R*,22*S*,23*R*)-**4** (red) and (3*S*,5*S*,8*R*,9*S*,10*R*,13*R*,14*R*,17*R*,22*R*,23*S*)-**4** (gray).

21/C-20 suggested the presence of a terminal double bond at C-20(21). The HMBC correlations from the olefinic proton (δ 6.06, H-24) to CH$_3$-26 (δ 20.7) and C-27 (δ 172.4) as well as from H$_3$-26 to C-25 and C-27 supported the presence of a trisubstituted double bond. The geometry of this Δ^{24} olefinic bond was determined as *Z* based on the NOESY correlation of H$_3$-26/H-24. The experimental value of $r_{H-21b/Me-30}$ was calculated to be 2.08 Å (Figure S5N, Supporting Information), using the NOE cross-peak volume and atomic distance of H-1β/H-19b as a reference, which was found to be closely comparable to that of **9**. Hence, the absolute configuration of C-17 was identified as *R*. From the above evidence, compound **5** was elucidated as (17*R*)-3,19-epoxy-dammara-20,24(*Z*)-diene-27-oic acid and given the trivial name (*Z*)-rhuslactic acid, analogous to the 17β-pair semialactone and semialactic acid.[7] Notably, **5** possesses a distinctive 3,19-hemiketal bridge in the A ring similar to compounds **1**−**4** and **9**. Up to the present, only 12 triterpenoids possessing a 3,19-hemiketal bridge in the A ring have been discovered from the family Anacardiaceae (Figure S11, Supporting Information).[5−7,17−20]

A sodium adduct ion peak at m/z 475.3181 (calcd 475.3188) in the HRESIMS of **6** supported its molecular formula as $C_{30}H_{44}O_3$, one oxygen less than that of **9**. The ^1H and ^{13}C NMR data of these two compounds were also similar. The only difference was that the characteristic hemiketal group in **9** was replaced by a new carbonyl group (δ 218.2) and an additional methyl group (δ 16.2). The HMBC correlations between H_2-1/H_2-2/H-5/H_3-28/H_3-29 and the carbonyl carbon (δ 218.2) supported the location of the carbonyl group at C-3, and those from H_3-19 to C-1, C-5, C-9, and C-10 were used to locate the methyl group at C-10. A similar experimental distance of H-21b/Me-30 (1.98 Å, Figure S6N, Supporting Information) to that in **9** was consistent with a 17R configuration in **6**. Comparison of the ECD spectra of **6** and **9** (Figure 4B) was used to define the absolute configurations of C-17 and C-22, which were the same as those of **9**. Hence, the structure of **6** was elucidated as (17R,22S)-3-oxodammara-20,24-dien-27,22-lactone, and this compound has been named rhuslaketone.

The molecular formula of **7** was assigned as $C_{30}H_{48}O_3$ from the sodium adduct ion occurring at m/z 479.3495 (calcd 479.3501), with seven degrees of unsaturation. The NMR data of the A−D rings of both compounds **6** and **7** were almost identical. The only differences were on their side chains. Similar to **6**, a carbonyl group in **7** could be located at C-3 from the HMBC cross-peaks of H_2-1/H_2-2/H-5/H_3-28/H_3-29 and the carbonyl carbon (δ 218.4). In addition, HMBC correlations of H-17/C-13, C-20; H_2-21/C-20, C-22; H-24/C-22, C-23, C-26, C-27; H_2-26/C-24, C-25, C-27; and H_2-27/C-25, C-26 revealed that the side chain of **7** is a 2-(pent-4-en-1-ylidene)propane-1,3-diol unit. Thus, the planar structure of **7** was determined as 26,27-dihydroxy-dammara-20,24-diene-3-one (Figure 5). The relative configuration of C-17 in **7** was established as described for compounds **1**−**6**, by calculating the dynamic distance of H-21b/Me-30 in the 17α-and 17β-side chains, respectively. DFT calculations of optimization and frequency of the 17α-and 17β-side chains were performed, and the theoretical $r_{H-21/Me-30}$ were calculated as 2.26 and 4.44 Å, respectively (Table S3, Supporting Information). The experimental value of $r_{H-21/Me-30}$ was 2.41 Å, referenced to the NOE cross-peak volume (a_{ref}) and atomic distance (r_{ref}, 2.46 Å) of H-12β/H-13β (Figure S7K, Supporting Information). The experimental value of $r_{H-21/Me-30}$ matched closely the theoretical one of a 17α-side chain, which was also quite similar to that of **9**. Based on the above analysis, compound **7** was proposed as (17R)-26,27-dihydroxydammara-20,24-diene-3-one and has been named rhuslaketodiol.

Compound **8** gave the same molecular formula as **7** from a $[M + Na]^+$ ion at m/z 479.3495 (calcd 479.3501) in the HRESIMS. Comparison of the ^1H and ^{13}C NMR and DEPT-135 spectra of **8** with those of **7** indicated that the differences between them were due to the absence of an exomethylene group and the presence of a tetrasubstituted double bond and a vinyl methyl group in the side chain of **8**. The planar structure of **8** could be constructed as 21,27-dihydroxydammar-17(20),24-dien-3-one via HMBC correlations of H-13, H_2-16, H_2-21, H_2-22/C-17; H_2-21, H_2-22/C-20; H-13, H_2-21/C-22; H_2-22/C-20; H_2-23/C-22, C-24; H-24/C-26; H_2-27/C-24; and H_3-26, H_2-27/C-25. Furthermore, a NOE cross-peak of H-24/H_3-26 confirmed that C-27 is hydroxylated and the geometry of the Δ^{24} olefinic bond is Z (Figure 5). Accordingly, the structure of **8** was determined as (24Z)-21,27-dihydrox-

ydammara-17(20),24-dien-3-one, and it has been named as rhuslaketonol.

Although a large number of dammarane triterpenoids have been found in Nature, the phytochemical investigation of *R. chinensis* resulted in eight new dammarane triterpenoids (**1**−**8**), of which **1**−**7** possess an unusual 17α-side chain. Also, **1**−**4** and **6** contain a 3-methyl-5,6-dihydro-2H-pyran-2-one moiety, and **1**−**5** have a distinctive 3,19-hemiketal structure bridge over the A ring. The uncommon structural fragments of the isolates inspired us to speculate on their biosynthetic pathways from a common precursor, 17α-dammarenediol-II,[24] which are described in detail in the Supporting Information (Scheme S1).

Preventive Effects of the Isolates on Zebrafish Heart Failure and Thrombosis. All the compounds with over 98% purity (**1**, **2**, and **4**−**9**) were subjected to the bioassays using zebrafish. Among them, compounds **1**, **2**, and **4**−**8** did not cause any adverse response in zebrafish at a concentration of 0.5 μg/mL, whether used alone or in combination with an inducer (verapamil or ponatinib). However, when cotreating zebrafish with 0.5 μg/mL of **9** along with the inducers, no blood flow was detected, despite **9** being nontoxic when administrated alone. Thus, the new compounds **1**, **2**, and **4**−**8** were selected for the assessments of preventive effects on zebrafish heart failure and thrombosis at 0.5 μg/mL. The results revealed that the compounds tested exhibited significant preventive effects on zebrafish heart failure (Figures 7 and 8 and Tables 4 and 5), while **7** and **8** showed no preventive effects. It is worth noting that **1**, **2**, and **4**−**6** significantly reduced the areas of pericardial edema and venous congestion (Figure 7), while increasing blood flow velocity (BFV, Figure 8B) and especially cardiac output (CO, Figure 8A) as well as heart rate (HR, Figure 8C) ($p < 0.001$). CO is an important index in the evaluation of cardiac ejection function. It may be implied that **1**, **2**, and **4**−**6** have the potential to meliorate structural cardiac lesions as well as the preload and postload of the heart, which have important influences on CO.[25] Notably, **1** and **4**−**6** exhibited significant preventive effects on zebrafish heart failure at 0.5 μg/mL ($p < 0.001$).

In order to further evaluate their preventive efficacies, compounds **1**, **2**, and **4**−**6** were compared with six first-line heart failure therapeutic drugs (Entresto, enalapril, digoxin, metoprolol, hydrochlorothiazide, and irbesartan) at the same or even higher concentrations (Table 5). These six clinical drugs were previously tested in the same zebrafish heart failure model with an identical protocol.[14] As an angiotensin II receptor−neprilysin inhibitor, Entresto shows a therapeutic efficacy superior to the standard heart failure drug enalapril (an angiotensin-converting enzyme inhibitor) in reducing cardiovascular death and hospitalization. Entresto was approved by the FDA in 2015 and by the NMPA in 2017. Digoxin is an adenosine diphosphate inhibitor; metoprolol is a β-blocker, which is used to lower the risk of heart failure death and hospitalization; hydrochlorothiazide is a diuretic medicaton;[26] and irbesartan is an angiotensin II receptor antagonist.[27] As shown in Table 5, compounds **1**, **4**, and **5** (0.5 μg/mL) displayed better effects on improving pericardial edema, venous congestion, CO, and BFV than enalapril (10 μg/mL), metoprolol, and irbesartan (0.5 μg/mL). Particularly, **5** performed better than all six clinical drugs in increasing CO and BFV. Moreover, the preventive effect of **5** on reducing heart dilatation was second only to Entresto (0.5 μg/mL), and
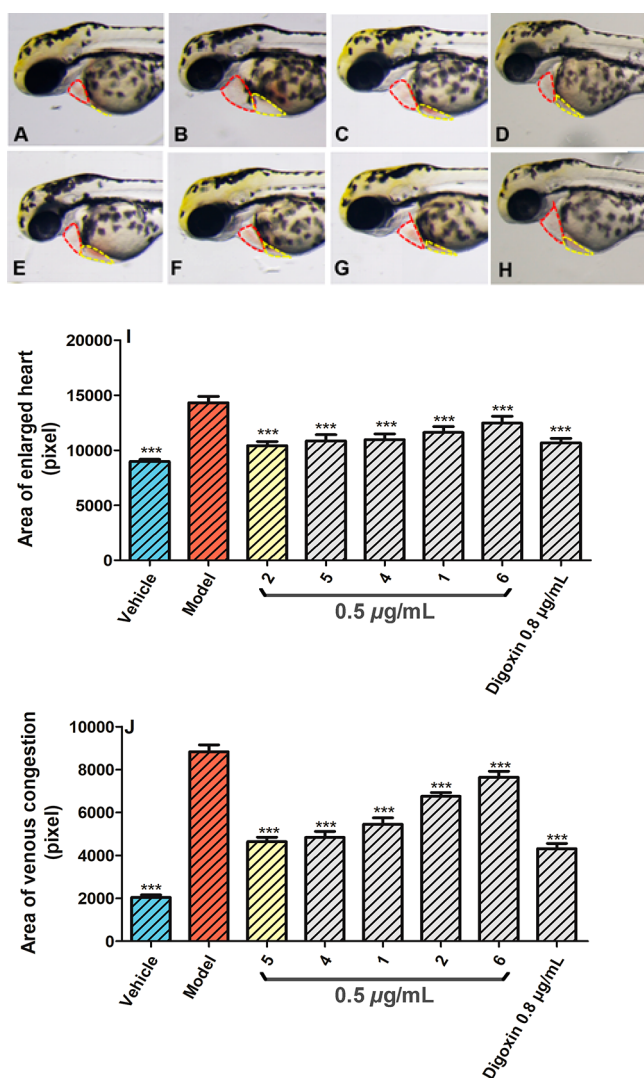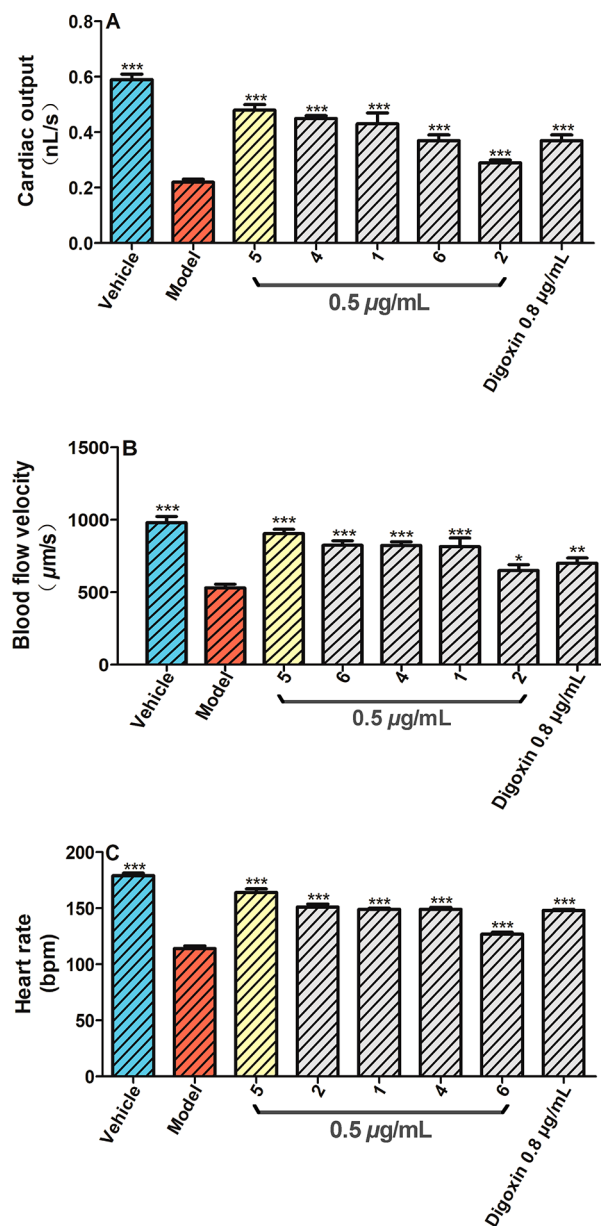
Figure 7. Reduced heart dilatation and venous congestion in a zebrafish heart failure model after treatments with **1**, **2**, and **4−6** at 0.5 μg/mL for 4.5 h. Heart and heart dilatation were marked in red, with venous and venous congestion in yellow. (A) Vehicle control; (B) model (zebrafish treated with 200 μM verapamil alone); (C−H): zebrafish treated with positive control digoxin (0.8 μg/mL) and compounds **1**, **2**, and **4−6**, respectively. The evaluation of the preventive effects of the tested compounds was based on quantitative results of area measurements of heart dilation (I) and venous congestion (J). Compared with model: ***$p < 0.001$.

Figure 8. Increase of cardiac output (A), blood flow velocity (B), and heart rate (C) in a heart failure zebrafish model after treatment with compounds **1**, **2**, and **4−6** at 0.5 μg/mL for 4.5 h. Compared with model: *$p < 0.05$, **$p < 0.01$, ***$p < 0.001$.

that on reducing venous congestion was just behind Entresto and digoxin (0.5 μg/mL).

In the assay used to evaluate preventive effects on zebrafish thrombosis, the heart red blood cell (RBC) intensity, which is suggested to inversely correlate with the thrombus severity, was used to quantify thrombosis.[15] As presented in Figure 9, compounds **1**, **2**, and **6** increased the RBC intensity, indicating reduced thrombosis in zebrafish. The preventive efficiency on thrombosis was 68%, 76%, and 65% for **1**, **2**, and **6**, respectively ($p < 0.001$).

In summary, among the compounds tested, **1**, **2**, and **4−6** demonstrated significant preventive effects on zebrafish heart failure. Further, **1**, **2**, and **6** also showed promising preventive activities on thrombosis. Overall, the most effective compound in the heart failure model was **5**, and the highly bioactive compound **1** was efficacious in both models, with effects comparable to or even better than the positive controls ($p < 0.001$); these two compounds may be considered as promising lead compounds toward the alleviation of cardiovascular disease.

■ EXPERIMENTAL SECTION

General Experimental Procedures. Optical rotations were acquired on an Autopol VI automatic polarimeter (Rudolph, Wilmington, DE, USA). UV and IR spectra were obtained on a Hitachi U-2900E (Hitachi, Tokyo, Japan) and an Avatar 360 ESP FTIR (Thermo Scientific, Waltham, MA, USA) spectrometer, respectively. ECD data were recorded on a JASCO-810 spectropolarimeter (JASCO, Japan). 1D and 2D NMR spectra were generated from a Bruker DRX-500 spectrometer (Bruker Biospin AG, Fallanden, Germany). Chemical shifts are expressed in δ (ppm) referenced to the solvent signals, and coupling constants are in J (Hz). HRESIMS were

Table 4. Areas of Enlarged Heart and Venous Congestion, Cardiac Output, Blood Flow Velocity, Heart Rate, and RBC Intensity in Zebrafish Treated with 1, 2, and 4−6 (0.5 µg/mL)[a]

sample	dosages (µg/mL)	area of enlarged heart (pixel)	area of venous congestion (pixel)	cardiac output (nL/s)	blood flow velocity (µm/s)	heart rate (bpm)	RBC intensity (pixel)
vehicle		8970 ± 211[d]	2046 ± 111[d]	0.59 ± 0.00[d]	980 ± 43[d]	179.0 ± 2.20[d]	3589 ± 226[d]
model		14 331 ± 568	8833 ± 320	0.22 ± 0.01	531 ± 24	114.0 ± 2.40	1989 ± 92
digoxin	0.8	10683 ± 399[d]	4317 ± 242[d]	0.37 ± 0.02[d]	700 ± 37[c]	148.0 ± 1.0[d]	
aspirin	45.0						3371 ± 191[d]
1	0.5	11 613 ± 548[d]	5457 ± 294[d]	0.43 ± 0.04[d]	815 ± 59[d]	149.0 ± 1.0[d]	3107 ± 157[d]
2	0.5	10 413 ± 389[d]	6753 ± 178[d]	0.29 ± 0.01[d]	651 ± 40[b]	151.0 ± 2.7[d]	3202 ± 200[d]
4	0.5	10 968 ± 523[d]	4843 ± 279[d]	0.45 ± 0.01[d]	823 ± 25[d]	149.0 ± 1.8[d]	2147 ± 114
5	0.5	10 846 ± 564[d]	4642 ± 203[d]	0.48 ± 0.02[d]	905 ± 29[d]	164.0 ± 3.2[d]	2369 ± 202
6	0.5	12 473 ± 627[d]	7644 ± 277[d]	0.37 ± 0.02[d]	824 ± 32[d]	127.0 ± 1.6[d]	3047 ± 212[d]

[a]Data are presented as means ± SE ($n = 3$). Digoxin and aspirin were ultilized as positive controls in the assessment of the preventive effects of zebrafish heart failure and thrombosis, respectively. [b]$*p < 0.05$ compared with model. [c]$**p < 0.01$ compared with model. [d]$***p < 0.001$ compared with model.

Table 5. Preventive Efficacy of 1, 2, and 4−6 (0.5 µg/mL) on Zebrafish Heart Failure and Thrombosis as Well as Their Comparison in Preventive Efficacy on Heart Failure with Six Clinical Cardiovascular Drugs Previously Tested with the Same Procedure[a]

sample	dosage (µg/mL)	efficacyon heart dilatation (%)	efficacyon venous congestion (%)	efficacyon cardiac output (%)	efficacy on blood flow velocity (%)	efficacy on heart rate (%)	preventive efficacy on thrombosis (%)
Data Obtained from This Study							
digoxin	0.8	68.00 ± 7.44[d]	67.00 ± 3.57[d]	41.00 ± 5.42[d]	38.00 ± 8.31[c]	52.00 ± 4.68[d]	
aspirin	45.0						86.00 ± 11.94[d]
1	0.5	66.00 ± 7.50[d]	51.00 ± 4.77[d]	58.00 ± 11.58[d]	65.00 ± 13.27[d]	60.00 ± 1.46[d]	68.00 ± 8.90[d]
2	0.5	73.00 ± 7.25[d]	31.00 ± 2.62[d]	22.00 ± 3.40[d]	27.00 ± 8.91[b]	57.00 ± 4.16[d]	76.00 ± 12.47[d]
4	0.5	63.00 ± 9.76[d]	59.00 ± 4.11[d]	64.00 ± 2.24[d]	65.00 ± 5.55[d]	54.00 ± 2.84[d]	10.00 ± 7.15
5	0.5	65.00 ± 10.51[d]	62.00 ± 2.99[d]	72.00 ± 7.15[d]	83.00 ± 6.41[d]	77.00 ± 4.89[d]	24.00 ± 12.60
6	0.5	55.00 ± 8.58[d]	23.00 ± 4.49[d]	41.00 ± 6.27[d]	67.00 ± 7.15[d]	27.00 ± 2.39[d]	65.00 ± 12.00[d]
Data Reported Previously[14]							
Entresto	0.5	90***	89***	65**	26**		
enalapril	10	31*	34*	34**	26**		
digoxin	0.5	53**	73***	40**	28**		
hydrochlo-rothiazide	0.5	56**	60***	53**	33*		
irbesartan	0.5	30*	36**	25*	15		
metoprolol	0.5	34**	29*	35***	17*		

[a]See the footnotes in Table 4. [b]$*p < 0.05$ compared with model. [c]$**p < 0.01$ compared with model. [d]$***p < 0.001$ compared with model.

acquired on a Bruker Daltonics micrOTOF-QII mass spectrometer (Bruker Daltonics, Bremen, Germany). LC-MS analyses were conducted using a Waters 2545 AutoPurification system equipped with a Waters SQ Detector II mass spectrometer and a Waters Sunfire C_{18} column (250 × 4.6 mm, 5 µm) (Waters, MA, USA). Semipreparative HPLC was performed with a Shimadzu system equipped with an SPD-M20A PDA detector (Shimadzu, Kyoto, Japan) and a Sedex 85 evaporative light-scattering detector (ELSD, Sedere, Alfortville, France). An Ultimate XS-C_{18} column (250 × 10 mm, 5 µm; Welch, Shanghai, People's Republic of China) was used for the final purification of compound **3**, and a Develosil ODS column (250 × 10 mm, 5 µm; Nomura Chemical, Seto-shi, Japan) was used for compounds **1**, **2**, and **4−8**. Silica gel (100−200 and 200−300 mesh, Qingdao Marine Chemical Inc., Qingdao, People's Republic of China), MCI gel CHP20/P120 (75−150 µm, Mitsubishi Chemical Industries, Tokyo, Japan), and a solid-phase extraction column (SPE, Strata C_{18}-E, Phenomenex, Torrance, CA, USA) were used for column chromatography (CC). TLC detections were conducted on silica gel plates (GF$_{254}$, 0.20−0.25 mm, Qingdao Marine Chemical Inc.). Spots were visualized using UV light (254 and 365 nm) and by spraying with 15% H_2SO_4/EtOH. The HPLC/MS grade solvents were from CNW (ANPEL, Shanghai, People's Republic of China). Purified water for semipreparative HPLC was prepared using a Millipore system (Bedford, MA, USA). The selected compounds for

efficacy assessment were at least 98% pure as detected by HPLC-ELSD as well as ^{1}H NMR spectroscopic analysis.

Plant Material. *Rhus chinensis* roots were collected in March 2017 from Dali City, Yunnan Province, People's Republic of China, and identified by Dr. Bo Fang (Yunnan Academy of Agricultural Sciences, Kunming, People's Republic of China). A voucher specimen (No. 20170310002) was deposited at the College of Pharmacy, Fujian University of Traditional Chinese Medicine.

LC-MS Analysis. Full details of the HPLC and MS conditions used are provided in the Supporting Information.

Extraction and Isolation. The dried roots of *R. chinensis* (43.0 kg) were refluxed with 95% aqueous MeOH (50 L × 4 h × 5) to afford a crude extract (6.6 kg), which was suspended in H_2O and partitioned with petroleum ether and EtOAc successively, to give petroleum ether (1.6 kg) and EtOAc (2.5 kg) portions. The EtOAc portion was subjected to silica gel CC, eluting with a gradient of CH_2Cl_2/MeOH (70:1−0:1) to provide 12 fractions (A−L). LC-MS analysis of the fractions suggested that Frs. D, E, G, and H (eluted with CH_2Cl_2/MeOH, 30:1, 15:1, 9:1, 7:1, respectively) might contain the desired triterpenoids, which were further separated. LC-MS detection combined with TLC analysis was used to track the targeted compounds. Fr. D (164.8 g) and Fr. E (35.7 g) were fractionated, respectively, by CC over silica gel, providing, in turn, nine (Frs. D1−D9) and four (Frs. E1−E4) subfractions, both using a gradient of CH_2Cl_2/MeOH (70:1, 30:1, 15:1, 5:1, 1:1) for elution. Fr. D5 (78.4
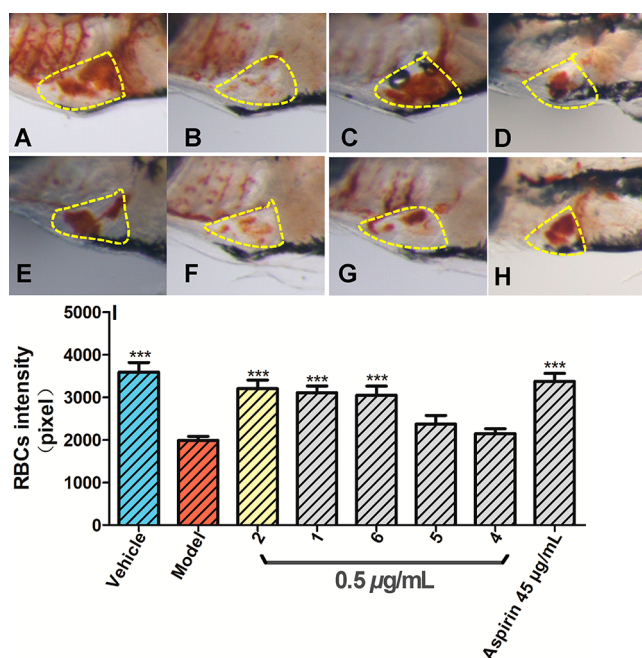
Figure 9. Increased heart RBC intensity in thrombotic zebrafish after being cotreated with 4 μg/mL ponatinib and the test compounds for 18 h. Hearts are marked in yellow. (A) Vehicle control; (B) model (zebrafish treated with ponatinib alone); (C–H) thrombotic zebrafish cotreated with the positive control aspirin (45 μg/mL) and compounds **1**, **2**, and **4–6** (0.5 μg/mL), respectively. (I) The preventive efficacy was measured based on quantitative image analysis of the heart RBC intensity in zebrafish. Compared with model: ***p < 0.001.

g) was chromatographed on silica gel CC (petroleum ether/Me$_2$CO, 6:1–2:1) to generate **9** (21.7 g). Fr. E2 (18.2 g) was separated by silica gel CC (petroleum ether/Me$_2$CO, 5:1–2:1) to obtain fractions E2-1–E2-14. Fr. E2-8 (570.0 mg) was purified further by MCI gel CC, using a gradient of MeOH/H$_2$O (70:30–100:0) as the mobile phase, giving E2-8-1–E2-8-13. Purification of E2-8-1 (50.3 mg), E2-8-9 (46.7 mg), and E2-8-10 (18.6 mg) by semipreparative HPLC (chromatographic conditions: 83% MeOH in H$_2$O for E2-8-1 and E2-8-9; 84% MeOH in H$_2$O for E2-8-10) yielded **8** (44.2 mg, t_R 34.8 min), **7** (37.2 mg, t_R 37.0 min), and **6** (5.2 mg, t_R 37.6 min), respectively. Fr. E3 (6.3 g) was fractionated by MCI gel CC (MeOH/H$_2$O, 90:10–100:0), affording fractions E3-1–E3-12. Subsequent separation of E3-2 (715.5 mg) by repeated CC over MCI gel (70–100% MeOH in H$_2$O), SPE (60–100% MeOH in H$_2$O), and ultimately semipreparative HPLC (48% CH$_3$CN in H$_2$O) afforded **4** (12.1 mg, t_R 67.0 min). Purification of Fr. E3-4 (374.3 mg) by MCI gel CC eluting with MeOH/H$_2$O (80:20–100:0) and subsequent semipreparative HPLC (60% CH$_3$CN in H$_2$O) resulted in the isolation of **2** (24.1 mg, t_R 37.0 min) and **1** (15.8 mg, t_R 43.5 min). Separation of Fr. G (137.5 g) was performed by silica gel CC, eluting with a gradient of CH$_2$Cl$_2$/MeOH (15:1–0:1), to give fractions G1–G11. Fr. G7 (20.3 g) was subjected to silica gel CC, with a gradient of petroleum ether/Me$_2$CO (5.5:2–1:1), to generate Fr. G7-1–Fr. G7-4. Fr. G7-2 (4.3 g) was loaded onto an MCI gel column, eluting with a gradient of increasing portions of MeOH (85–100%) in H$_2$O, to give fractions G7-2-1–G7-2-9. Compound **5** (80.5 mg, t_R 11.5 min) was finally purified from Fr. G7-2-5 (375.0 mg) by semipreparative HPLC (92% MeOH in H$_2$O). Fr. H (26.4 g) was separated by silica gel CC, using a gradient of increasing MeOH (5% to 100%) in CH$_2$Cl$_2$, giving Fr. H1–Fr. H12. Fr. H8 (1.8 g) was fractionated by MCI gel CC (70% to 100% MeOH in H$_2$O) to obtain fractions H8-1–H8-10. The further purification of Fr. H8-6 (52.3 mg) by semipreparative HPLC (72% MeOH in H$_2$O) furnished compound **3** (2.5 mg, t_R 17.5 min).

1β-Hydroxyrhuslactone (1): yellow, amorphous powder; $[\alpha]_D^{20}$ +13 (*c* 0.11, CHCl$_3$); ECD (*c* 1.01 mg/mL, CH$_3$CN) λ_{max} (Δε) 255 (−0.21), 199 (−2.09) nm; IR (film) ν_{max} 3404, 2923, 2851, 1634, 1589, 1472, 1417, 1385, 1367, 1125, 1043, 929, 864, 776 cm^{-1}; ^{1}H and ^{13}C NMR (CDCl$_3$, 500 MHz), see Tables 1 and 2; (+)-ESIMS *m/z* 507 [M + Na]$^+$; (+)-HRESIMS *m/z* 507.3076 [M + Na]$^+$ (calcd for C$_{30}$H$_{44}$O$_5$Na, 507.3086).

2β-Hydroxyrhuslactone (2): pale yellow, amorphous powder; $[\alpha]_D^{20}$ +23 (*c* 0.10, CHCl$_3$); ECD (*c* 1.00 mg/mL, CH$_3$CN) λ_{max} (Δε) 259 (−0.25), 199 (−4.03) nm; IR (film) ν_{max} 3442, 3359, 2921, 2851, 1654, 1637, 1584, 1472, 1422, 1387, 1325, 1125, 1041, 939, 859, 779 cm^{-1}; ^{1}H and ^{13}C NMR (CDCl$_3$, 500 MHz), see Tables 1 and 2; (+)-ESIMS *m/z* 507 [M + Na]$^+$; (+)-HRESIMS *m/z* 507.3076 [M + Na]$^+$ (calcd for C$_{30}$H$_{44}$O$_5$Na, 507.3086).

7β-Hydroxyrhuslactone (3): white, amorphous powder; ECD (*c* 0.50 mg/mL, CH$_3$CN) λ_{max} (Δε) 258 (−0.91), 198 (−10.16) nm; IR (film) ν_{max} 3354, 3195, 2923, 2853, 1706, 1634, 1475, 1417, 1248, 1198, 1183, 1133, 1078, 1021, 976, 906, 859, 816, 637 cm^{-1}; ^{1}H and ^{13}C NMR (CDCl$_3$, 500 MHz), see Tables 1 and 2; (+)-ESIMS *m/z* 507 [M + Na]$^+$; (+)-HRESIMS *m/z* 507.3076 [M + Na]$^+$ (calcd for C$_{30}$H$_{44}$O$_5$Na, 507.3086).

(23R)-23-Hydroxyrhuslactone (4): white, amorphous powder; $[\alpha]_D^{20}$ +86 (*c* 0.10, CHCl$_3$); ECD (*c* 0.06 mg/mL, CH$_3$CN) λ_{max} (Δε) 263 (−7.57), 226 (+24.31), 198 (−18.10) nm; IR (film) ν_{max} 3429, 2923, 2853, 1587, 1462, 1420, 1385, 1180, 1121, 1038, 929, 854, 776 cm^{-1}; ^{1}H and ^{13}C NMR (CDCl$_3$, 500 MHz), see Tables 1 and 2; (+)-ESIMS *m/z* 507 [M + Na]$^+$; (+)-HRESIMS *m/z* 507.3076 [M + Na]$^+$ (calcd for C$_{30}$H$_{44}$O$_5$Na, 507.3086).

(Z)-Rhuslactic acid (5): white, amorphous powder; $[\alpha]_D^{20}$ +36 (*c* 0.10, CHCl$_3$); IR (film) ν_{max} 3439, 3357, 2921, 2856, 1654, 1589, 1460, 1420, 1385, 1317, 1123, 1038, 926, 859, 781 cm^{-1}; ^{1}H and ^{13}C NMR (CDCl$_3$, 500 MHz), see Tables 1 and 2; (+)-ESIMS *m/z* 493 [M + Na]$^+$; (+)-HRESIMS *m/z* 471.3499 [M + H]$^+$ (calcd for C$_{30}$H$_{47}$O$_4$, 471.3474).

Rhuslaketone (6): white, amorphous powder; $[\alpha]_D^{20}$ +36 (*c* 0.13, MeOH); ECD (*c* 0.05 mg/mL, CH$_3$CN) λ_{max} (Δε) 259 (−0.88), 198 (−14.01) nm; IR (film) ν_{max} 3367, 2918, 2848, 1716, 1647, 1604, 1457, 1387, 1195, 1183, 1145, 1135, 1073, 1048, 1023, 976, 919, 679 cm^{-1}; ^{1}H and ^{13}C NMR (CDCl$_3$, 500 MHz), see Tables 1 and 2; (+)-ESIMS *m/z* 475 [M + Na]$^+$; (+)-HRESIMS *m/z* 475.3181 [M + Na]$^+$ (calcd for C$_{30}$H$_{44}$O$_3$Na, 475.3188).

Rhuslaketodiol (7): white, amorphous powder; $[\alpha]_D^{20}$ +28 (*c* 0.10, CHCl$_3$); IR (film) ν_{max} 3427, 2090, 1632, 1387, 1125, 694 cm^{-1}; ^{1}H and ^{13}C NMR (CDCl$_3$, 500 MHz), see Tables 1 and 2; (+)-ESIMS *m/z* 479 [M + Na]$^+$; (+)-HRESIMS *m/z* 479.3495 [M + Na]$^+$ (calcd for C$_{30}$H$_{48}$O$_3$Na, 479.3501).

Rhuslaketonol (8): white, amorphous powder; $[\alpha]_D^{20}$ +37 (*c* 0.10, CHCl$_3$); IR (film) ν_{max} 3409, 2921, 2851, 1589, 1387, 1121, 1041, 859, 776 cm^{-1}; ^{1}H and ^{13}C NMR (CDCl$_3$, 500 MHz), see Tables 1 and 2; (+)-ESIMS *m/z* 479 [M + Na]$^+$; (+)-HRESIMS *m/z* 479.3495 [M + Na]$^+$ (calcd for C$_{30}$H$_{48}$O$_3$Na, 479.3501).

Rhuslactone (9): white, needle crystals; $[\alpha]_D^{20}$ +34 (*c* 0.11, CHCl$_3$); ECD (*c* 1.17 mg/mL, CH$_3$CN) λ_{max} (Δε) 259 (−0.61), 199 (−7.15) nm; IR (film) ν_{max} 3362, 2923, 2853, 1719, 1657, 1634, 1472, 1377, 1125, 1096, 924, 856, 781, 754 cm^{-1}; ^{1}H and ^{13}C NMR (CDCl$_3$, 500 MHz), see Tables 1 and 2; (+)-ESIMS *m/z* 491 [M + Na]$^+$; (+)-HRESIMS *m/z* 491.3169 [M + Na]$^+$ (calcd for C$_{30}$H$_{44}$O$_4$Na, 491.3137).

Quantum Chemical Calculations. Confab was used to search the local low-energy conformers.[28] The generated conformers were further optimized by semiempirical method PM7[29] with MOPAC2016,[30] and the conformers in the 4 kcal/mol cutoff energy window were subjected to further DFT optimization. The optimization and frequency calculations were performed using the B3LYP/6-31G* level of theory. ^{13}C NMR spectroscopic data were calculated by the ωB97x-D/6-31G* level of theory in the gas phase. ECD calculations were performed using the B3LYP/6-311G* level of theory, and the ECD curves were simulated by SpecDis v1.71[31] with the sigma/gamma value of 0.35 eV. The calculated ^{13}C NMR, ECD data, and atomic distance of each conformers were Boltzmann-

averaged based on Gibbs free energy. All the DFT calculations were performed with the Gaussian09 software package.[32]

Preventive Efficacy Assessments on Zebrafish Heart Failure and Thrombosis. The efficacy assessment of the compounds in the zebrafish models was conducted by Hunter Biotechnology, Inc. (Hangzhou, People's Republic of China), which is accredited by the Association for Assessment and Accreditation of Laboratory Animal Care International[33,34] (AAALAC, accreditation number: 001458; Figure S13, Supporting Information) and the China National Accreditation Service for Conformity Assessment (CNAS, registration number: L12319). The maintenance of zebrafish has been reported previously.[14,15] Zebrafish treated with 200 μM verapamil for 0.5 h were employed as a heart failure model, and those treated with 4 μg/mL ponatinib for 18 h were used as a thrombosis model, with those including 0.1% DMSO used as vehicle control. Compounds **1**, **2**, and **4−8** were assayed for their preventive effects on heart failure and thrombosis in zebrafish at 0.5 μg/mL. The experimental procedure in the zebrafish heart failure model was conducted as reported,[14] while that for the thrombosis model was performed mainly using a literature method,[15] with some modifications. Briefly, 30 AB strain zebrafish of 5 dpf (days postfertilization) were distributed into six-well plates. After being cotreated with 4 μg/mL ponatinib[16] and the sample for 18 h, zebrafish thrombosis was quantified using a reported method.[15] The quantitative image analysis of the heart RBC intensity (described as S in the following calculation) was used to measure the preventive effect on thrombosis. Each experiment was repeated three times. One-way ANOVA followed by the Student's t test was utilized in the statistical analyses, and $p < 0.05$ was statistically significant. The efficacies on reducing heart dilatation and venous congestion, increasing CO, BFV, and HR, as well as that of preventing thrombosis were calculated by formulas 1 to 6. Formulas 1 to 6 are as follows: formula 1(2): efficacy (%) = $[A_{1(2)}(model) − A_{1(2)}(compound)]/[A_{1(2)}(model) − A_{1(2)}(vehicle)] \times 100\%$; formula 3: efficacy (%) = $[CO(compound) − CO(model)]/[CO(vehicle) − CO(model)] \times 100\%$; formula 4: efficacy (%) = $[BFV(compound) − BFV(model)]/[BFV(vehicle) − BFV(model)] \times 100\%$; formula 5: efficacy (%) = $[HR(compound) − HR(model)]/[HR(vehicle) − HR(model)] \times 100\%$; formula 6: efficacy (%) = $[S(compound) − S(model)]/[S(vehicle) − S(model)] \times 100\%$.

■ ASSOCIATED CONTENT

ⓈⒾ Supporting Information

The Supporting Information is available free of charge at https://pubs.acs.org/doi/10.1021/acs.jnatprod.9b00857.

> IR and NMR spectra, HRESIMS data, as well as the purity reports of **1−9**; structures and molecular weights of the reported triterpenoids from *R. chinensis* as well as those of triterpenoids with the 3,19-hemiketal structure in the A ring from the family Anacardiaceae; experimental conditions and results for the LC-MS detection of the EtOAc portion of *R. chinensis* roots; Boltzmann-averaged distances of H-21b/H$_3$-30 for **9a** and **9c**, as well as those for either 17-α or 17-β of **7**; detailed biosynthetic proposal for all the isolates; certificate of AAALAC accreditation for Hangzhou Hunter Biotechnology, Inc. (PDF)

■ AUTHOR INFORMATION

Corresponding Authors

Wei Xu − *College of Pharmacy and Centre of Biomedical Research & Development, Fujian University of Traditional Chinese Medicine, Fuzhou 350122, People's Republic of China*; Phone: +86 0591-22861693; Email: 2000017@fjtcm.edu.cn

Xu-Wen Li − *State Key Laboratory of Drug Research, Shanghai Institute of Materia Medica, Chinese Academy of Sciences, Shanghai 201203, People's Republic of China*; ⓞ orcid.org/ 0000-0001-7919-9726; Phone: +86 021-50806600; Email: xwli@simm.ac.cn

Authors

Miao Ye − *College of Pharmacy and Centre of Biomedical Research & Development, Fujian University of Traditional Chinese Medicine, Fuzhou 350122, People's Republic of China*; ⓞ orcid.org/0000-0002-9131-2207

Wen Xu − *College of Pharmacy and Centre of Biomedical Research & Development, Fujian University of Traditional Chinese Medicine, Fuzhou 350122, People's Republic of China*; ⓞ orcid.org/0000-0001-7126-8029

Da-Qing He − *College of Pharmacy and Centre of Biomedical Research & Development, Fujian University of Traditional Chinese Medicine, Fuzhou 350122, People's Republic of China*

Xian Wu − *College of Pharmacy and Centre of Biomedical Research & Development, Fujian University of Traditional Chinese Medicine, Fuzhou 350122, People's Republic of China*

Wen-Fang Lai − *College of Pharmacy and Centre of Biomedical Research & Development, Fujian University of Traditional Chinese Medicine, Fuzhou 350122, People's Republic of China*

Xiao-Qin Zhang − *College of Pharmacy and Centre of Biomedical Research & Development, Fujian University of Traditional Chinese Medicine, Fuzhou 350122, People's Republic of China*

Yu Lin − *College of Pharmacy and Centre of Biomedical Research & Development, Fujian University of Traditional Chinese Medicine, Fuzhou 350122, People's Republic of China*

Complete contact information is available at:
https://pubs.acs.org/10.1021/acs.jnatprod.9b00857

Author Contributions

⊥M. Ye and W. Xu are designated as the co-first authors of this paper, having made equal contributions to this work.

Notes

The authors declare no competing financial interest.

■ REFERENCES

(1) GBD 2017 Cause of Death Collaborators. *Lancet* **2018**, *392*, 1736−1788.
(2) Newman, D. J.; Cragg, G. M. *J. Nat. Prod.* **2016**, *79*, 629−661.
(3) Djakpo, O.; Yao, W. R. *Phytother. Res.* **2010**, *24*, 1739−1747.
(4) Shen, Y. Y. *Chin. Pharm. Bull.* **1980**, *5*, 28.

(5) Kim, G. S.; Jeong, T. S.; Kim, Y. O.; Baek, N. I.; Cha, S. W.; Lee, J. W.; Song, K. S. *J. Korean Soc. Appl. Biol. Chem.* **2010**, *53*, 417−421.

(6) Sung, C. K.; Akiyama, T.; Sankawa, U.; Iitaka, Y.; Han, D. S. *J. Chem. Soc., Chem. Commun.* **1980**, *19*, 909−910.

(7) Lee, I. S.; Oh, S. R.; Ahn, K. S.; Lee, H. K. *Chem. Pharm. Bull.* **2001**, *49*, 1024−1026.

(8) Gu, Q.; Wang, R. R.; Zhang, X. M.; Wang, Y. H.; Zheng, Y. T.; Zhou, J.; Chen, J. J. *Planta Med.* **2007**, *73*, 279−282.

(9) Tan, D. P.; Yan, Q. X.; Ma, X. J. *Chem. Nat. Compd.* **2015**, *51*, 542−543.

(10) Connolly, J. D.; Hill, R. A. *Nat. Prod. Rep.* **2001**, *18*, 560−578.

(11) Connolly, J. D.; Hill, R. A. *Nat. Prod. Rep.* **1995**, *12*, 609−638.

(12) Connolly, J. D.; Hill, R. A. *Nat. Prod. Rep.* **1994**, *11*, 467−492.

(13) Basu, S.; Sachidanandan, C. *Chem. Rev.* **2013**, *10*, 7952−7980.

(14) Zhu, X. Y.; Wu, S. Q.; Guo, S. Y.; Yang, H.; Xia, B.; Li, P.; Li, C. Q. *Zebrafish* **2018**, *15*, 243−253.

(15) Zhu, X. Y.; Liu, H. C.; Guo, S. Y.; Xia, B.; Song, R. S.; Lao, Q. C.; Xuan, Y. X.; Li, C. Q. *Zebrafish* **2016**, *13*, 335−344.

(16) Wang, M. L.; Pan, Y. M.; Jin, M.; Xu, X. P.; Wang, D. J.; Ma, Q. X.; Chen, M. L. *Acta. Lab. Anim. Sci. Sin.* **2016**, *24*, 432−438.

(17) Shin, H.; Park, Y.; Choi, J. H.; Jeon, Y. H.; Byun, Y.; Sung, S. H.; Lee, K. Y. *Magn. Reson. Chem.* **2017**, *55*, 763−766.

(18) Chiu, C. L.; Lee, T. H.; Shao, Y. Y.; Kuo, Y. H. *J. Asian Nat. Prod. Res.* **2008**, *10*, 684−688.

(19) Lee, T. H.; Chiou, J. L.; Lee, C. K.; Kuo, Y. H. *J. Chin. Chem. Soc.* **2005**, *52*, 833−841.

(20) Schmidt, J.; Porzel, A.; Adam, G. *Phytochemistry* **1998**, *49*, 2049−2051.

(21) Wang, W. X.; Kusari, S.; Laatsch, H.; Golz, C.; Kusari, P.; Strohmann, C.; Kayser, O.; Spiteller, M. *J. Nat. Prod.* **2016**, *79*, 704−710.

(22) Kutateladze, A. G.; Reddy, D. S. *J. Org. Chem.* **2017**, *82*, 3368−3381.

(23) Grimblat, N.; Zanardi, M. M.; Sarotti, A. M. *J. Org. Chem.* **2015**, *80*, 12526−12534.

(24) Tansakul, P.; Shibuya, M.; Kushiro, T.; Ebizuka, Y. *FEBS Lett.* **2006**, *580*, 5143−5149.

(25) Zhu, D. N.; Wang, H. T.; Luo, Z. Q.; Guan, Y. F.; Jin, X. R. *Physiology*, 8th ed.;People's Medical Publishing House: Beijing, 2013; pp 93−97.

(26) Yang, B. F.; Chen, J. G.; Zang, W. J.; Wei, M. J. *Pharmacology*, 9th ed.;People's Medical Publishing House: Beijing, 2018; pp 232−235.

(27) Yang, B. F.; Chen, J. G.; Zang, W. J.; Wei, M. J. *Pharmacology*, 9th ed.;People's Medical Publishing House: Beijing, 2018; p 207.

(28) O'Boyle, N. M.; Vandermeersch, T.; Flynn, C. J.; Maguire, A. R.; Hutchison, G. R. *J. Cheminf.* **2011**, *3*, 8.

(29) Stewart, J. J. P. *J. Mol. Model.* **2013**, *19*, 1−32.

(30) Stewart, J. J. P. *J. Mol. Model.* **2016**, *22*, 259.

(31) Bruhn, T.; Schaumlöffel, A.; Hemberger, Y.; Bringmann, G. *Chirality* **2013**, *25*, 243−249.

(32) Frisch, M. J.; Trucks, G. W.; Schlegel, H. B.; Scuseria, G. E.; Robb, M. A.; Cheeseman, J. R.; Scalmani, G.; Barone, V.; Petersson, G.; Nakatsuji, H.; Li, X.; Caricato, M.; Marenich, A.; Bloino, J.; Janesko, B. G.; Gomperts, R.; Mennucci, B.; Hratchian, H. P.; Ortiz, J. V.; Izmaylov, A. F.; Sonnenberg, J. L.; Williams-Young, D.; Ding, F.; Lipparini, F.; Egidi, F.; Goings, J.; Peng, B.; Petrone, A.; Henderson, T.; Ranasinghe, D.; Zakrzewski, V. G.; Gao, J.; Rega, N.; Zheng, G.; Liang, W.; Hada, M.; Ehara, M.; Toyota, K.; Fukud, R.; Hasegawa, J.; Ishida, M.; Nakajima, T.; Honda, Y.; Kitao, O.; Nakai, H.; Vreven, T.; Throssell, K.; Montgomery, J. A.; Peralta, J. J. E.; Ogliaro, F.; Bearpark, M.; Heyd, J. J.; Brothers, E.; Kudin, K. N.; Staroverov, V. N.; Keith, T.; Kobayashi, R.; Normand, J.; Raghavachari, K.; Rendell, A.; Burant, J. C.; Iyengar, S. S.; Tomasi, J.; Cossi, M.; Millam, J. M.; Klene, M.; Adamo, C.; Cammi, R.; Ochterski, J. W.; Martin, R. L.; Morokuma, K.; Farkas, O.; Foresman, J. B.; Fox, D. J. *Gaussian 09*, Version A.02; Gaussian, Inc.: Wallingford, CT, 2016.

(33) Li, J. L.; Zhou, J.; Chen, Z. H.; Guo, S. Y.; Li, C. Q.; Zhao, W. M. *J. Nat. Prod.* **2015**, *78*, 1548−1555.

(34) Duan, J. C.; Yu, Y.; Li, Y.; Li, Y. B.; Liu, H. C.; Jing, L.; Yang, M.; Wang, J.; Li, C. Q.; Sun, Z. W. *Nanotoxicology* **2016**, *10*, 575−585.